Applied Thermal Engineering 53 (2013) 278–284

Contents lists available at SciVerse ScienceDirect

Applied Thermal Engineering

journal homepage: www.elsevier.com/locate/apthermeng

Effects of contact resistance and metal additives in finned-tube adsorbent beds on the performance of silica gel/water adsorption chiller

A. Rezk, R.K. Al-Dadah*, S. Mahmoud, A. Elsayed

School of Mechanical Engineering, University of Birmingham, Birmingham Edgbaston, B15 2TT, United Kingdom

ARTICLE INFO

Article history:
Received 12 December 2011
Accepted 3 April 2012
Available online 18 May 2012

Keywords:
Adsorption chiller
Silica gel/water
Contact resistance
Metal additives

ABSTRACT

Recently interest in adsorption cooling systems has increased due to their capability to utilise low grade heat sources and environmentally friendly refrigerants. Currently, most of the commercially available adsorption cooling systems utilise granular packed adsorbent beds. Enhancing the heat transfer process inside the adsorbent bed will improve the overall efficiency of the adsorption system. Using recently developed empirical lumped analytical simulation model for a 450 kW two-bed silica gel/water adsorption chiller, this paper theoretically investigates the effects of various adsorbent bed heat transfer enhancement techniques on the adsorption system cooling capacity. Firstly, coating the first adsorbent layer to the metal part and packing the rest of adsorbent granules to eliminate the thermal contact resistance between heat exchanger metal and granules while keeping the same level of permeability. Secondly, adding metal particles to the adsorbent in order to enhance the granules thermal conductivity. The effective thermal conductivity of adsorbent/metal mixtures were determined and validated by comparing it with published experimental data. Also, the combined effect of using both techniques simultaneously was investigated. All these investigations were carried out at various adsorption bed fin spacing. Results of the combined techniques showed that the enhancement in the cooling capacity and system coefficient of performance (COP) increased with increasing the fin spacing ratio to reach maximum of 25% and 10% respectively at fin spacing ratio of 2.

1. Introduction

Adsorption cooling systems are increasingly used for applications where cooling is required and low grade heat is available [1]. They are applied in combined cooling, heating and power (CCHP) systems employed in many industrial and commercial applications [2] and in sustainable building climatisation using solar energy as heat source [3,4]. Several adsorption pairs were evaluated and silica gel/water has shown significant advantages in terms of thermal performance and environmental impact [5]. Although water refrigerant is considered in chilling applications only, it has excellent thermo-physical properties of high latent heat of evaporation, high thermal conductivity, low viscosity, thermally stable in wide range of operating temperatures and the compatibility with wide range of materials. Silica gel as water vapour adsorbent has the advantages of high adsorption/desorption rate, low generation heat and low generation temperature.

Many commercially available adsorption cooling systems use granular packed adsorbent bed design. Such type of adsorbent bed has the advantage of high mass transfer performance due to the high permeability level [6], but it has the drawbacks of poor heat transfer performance where; high contact thermal resistance between adsorbent granules and heat exchanger metal surface [7], discontinuity of heat transfer through granules due to the voids in-between the granules [8] and poor thermal conductivity of the commonly used physical adsorbents. Therefore many methods were investigated to enhance the heat transfer performance of adsorbent material such as mixing adsorbent granules with metal additives to improve their thermal conductivity [9], coating the bed heat exchanger metal with all the adsorbent to eliminate the contact thermal resistance [7], covering adsorbent granules by polyaniline net [9], adsorbent deposition over metallic foam [6] and using consolidated bed techniques (compressed granules and clay [9], using expandable graphite [10], moulding granules and binder addition [11] and adsorbent granules and metal foam [12]). Most of these methods improve the heat transfer performance of adsorbent material but reduce its mass transfer performance [13].

Modelling is an effective tool for the design of adsorption cooling systems [14]. A recently constructed and validated empirical lumped analytical simulation model based on the fundamental

* Corresponding author. Tel.: +44 (0) 121 4143513.
E-mail address: r.k.al-dadah@bham.ac.uk (R.K. Al-Dadah).

1359-4311
doi:10.1016/j.applthermaleng.2012.04.008

heat and mass transfer equations was developed [5]. In such model the overall heat transfer conductance was calculated using empirical correlations taking into account the operating conditions and the geometry of heat exchangers. Thus, the model can be used to predict the effect of changing physical and operating conditions on chiller performance [15].

This paper evaluates some of the methodologies used to enhance the heat transfer performance of the adsorbent in terms of improving the bed thermal performance and the overall cooling capacity of the adsorption system. Firstly, coating the first adsorbent layer to the metal surface and packing the rest of adsorbent granules to eliminate the thermal contact resistance between heat exchanger metal and granules while keeping the same level of permeability. Secondly, adding various metal additives to the adsorbent in order to enhance its thermal conductivity. Finally, the combined effect of using both techniques simultaneously was investigated. All these investigations were carried out using fixed bed dimensions but at various fin spacing.

2. System description

Fig. 1 shows schematic diagram of the simulated two-bed adsorption chiller. Each adsorbent bed is connected to the evaporator or condenser by flap valves operated by the effect of pressure difference between heat exchangers during adsorbing or desorbing respectively. On the other hand, the flow of cooling and heating water to the adsorber and desorber respectively, flow of the chilled water through the evaporator and flow of cooling water to the condenser are controlled by 12 pneumatic valves.

Physically, the adsorbent bed heat exchanger is constructed from plain copper tubes with aluminium rectangular fins and the silica gel granules are packed to fill the gaps between fins, shown in Fig. 2. The adsorbent bed is covered by a metal mesh to prevent the falling of silica gel granules. These adsorbent beds are installed in two-bed silica gel/water adsorption chiller incorporating mass and heat recovery schemes. The operation modes and secondary flow valving control method were presented in details in [15].

3. Simulation model

The simulation model of the adsorption system was constructed from four sub-models describing the heat and mass transfer performance of evaporator, condenser, adsorber and desorber. The four sub-models were linked together taking into account the various operating modes. Eqs. (1)–(3) present the energy balance equations for adsorbent bed, evaporator and condenser respectively, where the adsorbent, adsorbate and heat exchanger metal are assumed to be individually momentarily at the same temperature. Eq. (4) presents the refrigerant mass balance in the evaporator taking into account no flow condition in case of heat and mass recovery.

$$\begin{aligned}&\left(\zeta M_{\mathrm{bed-w}}C_{\mathrm{w}}(T_{\mathrm{bed}})+M_{\mathrm{sg}}w_{\mathrm{sg}}\mathrm{Cp}_{\mathrm{ref}}(T_{\mathrm{bed}})+M_{\mathrm{sg}}C_{\mathrm{sg}}\right.\\&\left.+M_{\mathrm{bed-met}}C_{\mathrm{bed-met}}\right)\mathrm{d}T_{\mathrm{bed}}/\mathrm{d}t\\&=(1-\zeta)\sum_{n=1}^{n=N_{\mathrm{bed}}}dUA_{\mathrm{bed}-n}\times\mathrm{LMTD}_{\mathrm{bed}}+(\phi\bullet\partial)\left[\gamma\left\{h_{\mathrm{g}}(T_{\mathrm{Hex}})\right.\right.\\&\left.-h_{\mathrm{g}}(P_{\mathrm{Hex}},T_{\mathrm{bed}})\right\}+(1-\gamma)\left\{h_{\mathrm{g}}(P_{\mathrm{Hex}},T_{\mathrm{Hex}})-h_{\mathrm{g}}(P_{\mathrm{bed}},T_{\mathrm{bed}})\right.\\&\left.\times\right\}\left]M_{\mathrm{sg}}\mathrm{d}w_{\mathrm{sg}}/\mathrm{d}t+\phi M_{\mathrm{sg}}\Delta H_{\mathrm{sg}}\mathrm{d}w_{\mathrm{sg}}/\mathrm{d}t\right.\end{aligned}\tag{1}$$

$$\begin{aligned}&\left[\mathrm{Cp}_{\mathrm{ref,f}}(T_{\mathrm{evap}})M_{\mathrm{ref,evap}}+C_{\mathrm{evap-met}}M_{\mathrm{evap-met}}\right]\mathrm{d}T_{\mathrm{evap}}/\mathrm{d}t\\&=\mathrm{UA}_{\mathrm{evap}}\times\mathrm{LMTD}_{\mathrm{evap}}+\phi\left[h_{\mathrm{ref,evap,in}}\right.\\&\left.-h_{\mathrm{ref,evap,out}}\right]M_{\mathrm{sg}}\mathrm{d}w_{\mathrm{sg}}/\mathrm{d}t+\mathrm{d}E_{\mathrm{pump}}/\mathrm{d}t\end{aligned}\tag{2}$$

$$\begin{aligned}&\left[\mathrm{Cp}_{\mathrm{ref,l}}(T_{\mathrm{cond}})M_{\mathrm{ref,cond}}+C_{\mathrm{cond-met}}M_{\mathrm{cond-met}}\right]\mathrm{d}T_{\mathrm{cond}}/\mathrm{d}t\\&=\mathrm{UA}_{\mathrm{cond}}\times\mathrm{LMTD}_{\mathrm{cond}}+\phi\left[\left(h_{\mathrm{ref,cond,l}}-h_{\mathrm{ref,cond,g}}\right)\right.\\&\left.+\mathrm{Cp}_{\mathrm{ref}}(T_{\mathrm{cond}}-T_{\mathrm{bed}})\right]M_{\mathrm{sg}}\mathrm{d}w_{\mathrm{sg}}/\mathrm{d}t\end{aligned}\tag{3}$$

$$\mathrm{d}M_{\mathrm{ref,f,evap}}/\mathrm{d}t=-\phi\cdot M_{\mathrm{sg}}(\mathrm{d}w_{\mathrm{des}}/\mathrm{d}t+\mathrm{d}w_{\mathrm{ads}}/\mathrm{d}t)\tag{4}$$

where M, C, Cp, T, LMTD, P, h, w, ΔH_{ads} and t are the mass, specific heat, specific heat at constant pressure, temperature, log mean temperature difference, pressure, specific enthalpy, uptake value, isosteric heat of adsorption, and time respectively. The subscripts bed, evap and cond refer to adsorbent bed (ads/des), evaporator and condenser condition respectively and w, sg, ref and met refer to water, silica gel, refrigerant and metal respectively. Subscripts g, f, refer to fluid vapour and liquid condition respectively and Hex

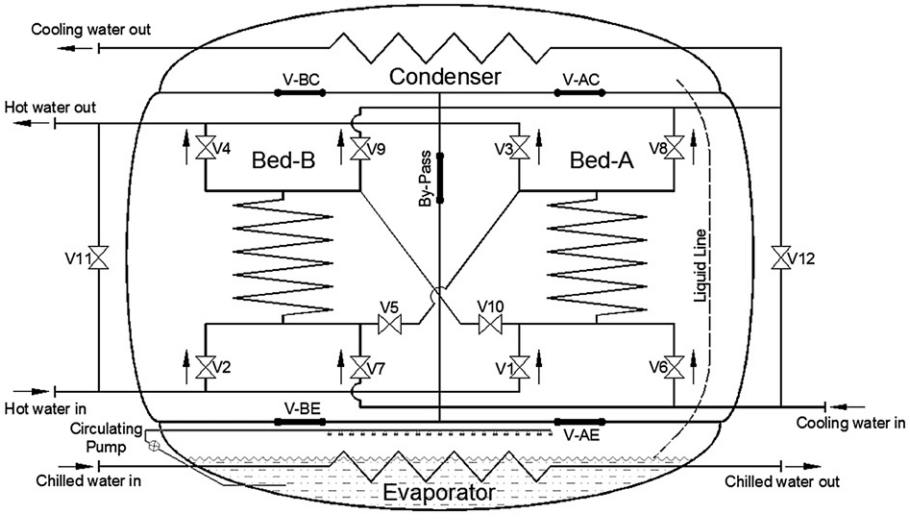

Fig. 1. Schematic diagram for simulated two-bed cycle adsorption heat pump.

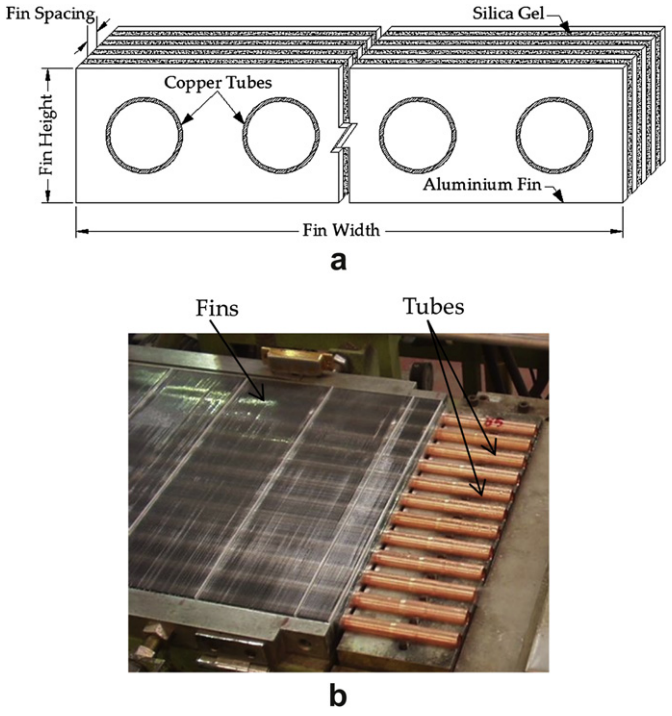

Fig. 2. (a) Schematic diagram of finned-tube adsorbent bed, (b) Pictorial view of the adsorbent bed.

refers to the heat exchanger that interconnect with the adsorbent bed. A group of flags $(\zeta, \phi, \partial, \gamma)$ were used to enable or disable some of the equation terms based on the operating mode as shown in Table 1. The rate of adsorption was evaluated using linear driving force kinetic model (LDF), where water vapour can reach all silica gel granules and the inter-particle mass transfer resistance can be neglected, Eq. (5).

$$\frac{dw}{dt} = \left(15D_{so}/R_p^2\right)\exp(-E_a/RT)\left(w^* - w\right) \quad (5)$$

where R_p (m), D_{so}, E_a, and w^* are particles radius, pre-exponential constant, activation energy, universal gas constant and equilibrium uptake respectively. Table 2 presents different constants values. The model was validated using experimental measurements from 450 kW commercial water chiller with maximum absolute percent deviation of 17.8% [5].

4. Effect of contact thermal resistance on chiller performance at various fin spacing

Enhancing the adsorption kinetics is necessary in order to improve the adsorption chiller performance. Using the same adsorbent/adsorbate pair, enhancing adsorption kinetics can be achieved by enhancing both heat and mass transfer performance. In packed finned-tube adsorbent bed design increasing the overall heat transfer coefficient U and heat transfer area A increase the overall heat transfer conductance UA and hence the adsorption kinetics. Fig. 3(a) shows the control volume of a typical element from the adsorber bed. It includes one fin attached to the copper tube at the base which is in contact with the secondary fluid at temperature (T_w). The fin is surrounded by silica gel from both sides and water vapour above it at (T_{bed}). During the heat transfer from/to the secondary fluid to/from adsorbent bed surface in desorption/adsorption mode, there are six heat transfer resistances namely; (1) radial convective thermal resistance from the secondary fluid stream to the internal tube wall R1, (2) radial conduction thermal resistance through tube wall R2, (3) two contact thermal resistances between silica gel granules and tube outside surface and fins surface R3 and R4 in both radial and axial directions respectively and (4) two conduction thermal resistances through silica gel granules in radial and axial direction R5 and R6, shown schematically in Fig. 3(b). The axial conductive thermal resistance through the tube wall and metal–metal contact thermal resistance between tube wall and aluminium fins were neglected due to their insignificant effect compared by the aforementioned thermal resistances. In Fig. 3, htc, A, d, k, R_{cont} and δ are convection heat transfer coefficient, surface area, diameter, thermal conductivity, contact thermal resistance and adsorbent layer thickness respectively. Subscripts i, o, t, f, s, ads and r refer to inside, outside, tube, fin, surface, adsorbent and root diameter respectively. The parameters that affect the heat and mass transfer through the adsorbent bed ranked based on their importance are the adsorbent bed permeability, thermal contact resistance between adsorbent granules and heat exchanger metal surface and adsorbent layer thermal conductivity [16,17].

Generally, thermal contact resistance between silica gel granules and heat exchanger metal surface (tubes and fins) represents averagely 25% of the overall heat transfer resistance. Adsorbent bed

Table 1
Simulation model switching flags.

Mode	ζ	ϕ	∂	γ
Ads-evaporation	0	1	1	1
Des-condensation	0	1	0	0
Mass recovery	1	0	1	0
Heat recovery	0	0	1	0

Table 2
Parameters value of the simulation model [15].

Constant	Value
D_{so}	3.625E-3
E_a	4.2 E4
R_p	0.16 E-3
ΔH_{ads}	2.939 E6

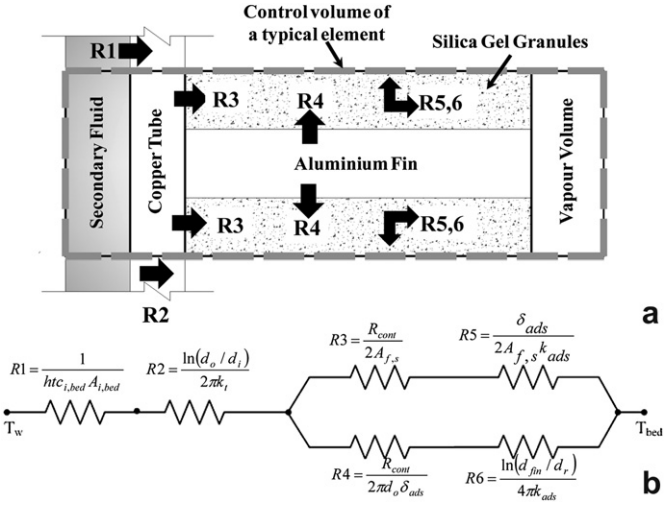

Fig. 3. (a) Control volume of an element in the adsorber bed, (b) Heat transfer resistance schematic diagram.

coating techniques were used to eliminate the thermal contact resistance of various adsorbents and bed designs [18–23]. The disadvantage of the techniques used is the dramatic reduction in adsorbent bed permeability which counteracts any improvement due to reducing the contact thermal resistance. Also, the coated adsorbent layer is usually within few millimetres which dramatically increase the bed heat exchanger metal mass and reduces the heat capacity ratio (HCR) defined as the silica gel heat capacity over the adsorbent-bed metal heat capacity, Eq. (6). Using bed coating technique, it is recommended to use granules of relatively larger size [20]. However the larger the granules size, the worse the adsorption kinetics, where the adsorption rate is inversely proportional to the squared average granules radius. Therefore, this work investigates the effect of gluing the first layer of the silica gel and packing the rest at various fin spacing. It is expected that this will eliminate the contact resistance while maintaining the permeability of the silica gel bulk. Fig. 4 shows the effect of eliminating the contact resistances (R3 and R4 equal zero) on the adsorbent-bed thermal performance (4(a)) and the overall system performance (4(b)) at various fins spacing ratio (FSR). The FSR is the value of fin spacing relative to its design value. In Fig. 4(a), the heating capacity ratio (HCR) and the number of thermal units (NTU) as defined in Eq. (7) are used to describe the adsorbent-bed thermal performance.

$$\mathrm{HCR} = M_{sg}C_{sg}/M_{met}C_{met} \tag{6}$$

$$\mathrm{NTU} = \mathrm{UA}_{bed}/\dot{m}_{w}C_{w} \tag{7}$$

where M, C, U, A, $\dot{m}$ are mass, specific heat capacity, overall heat transfer coefficient, heat transfer surface area and mass flow rate. The subscripts sg, met and w stand for silica gel, metal and water respectively. Results show that eliminating the contact resistance increased the adsorbent bed heat exchanger NTU without changing the bed HCR. At fin spacing ratio of 2, the NTU increased by 25.3% and 31.0% for heating and cooling respectively. On the other hand, at fin spacing ratio of 0.8, the NTU increased by 24.2% and 47.1% for heating and cooling respectively. In Fig. 4(b) the cooling capacity, heating capacity and coefficient of performance (COP) are used to describe the overall system performance. The cooling capacity indicates the rate of cooling produced by the chiller and the heating capacity measures the rate of heat required to drive the desorption process. The COP is the ratio between the cooling and the heating capacities. It can be seen from this Figure that eliminating the contact resistance increased the system cooling capacity, heating capacity and COP. At fin spacing ratio of 2, the cooling capacity, heating capacity and COP increased by 12.1%, 7.5% and 4.2% respectively. On the other hand, at fin spacing ratio of 0.8, the cooling capacity, heating capacity and COP increased by 5.0%, 1.0% and 4.0%. Eliminating or reducing the contact resistance will increase the overall heat transfer between the silica gel and the secondary fluid (U in Eq. (7)). This will lead silica gel to operate under lower or higher temperature limits thus improving the efficiency of the adsorption/desorption processes and increasing the refrigerant flow rate which in turn increase the system cooling capacity, heating capacity and COP.

5. Effect of metal additives

Research has shown that adding metal particles to adsorbent materials enhance their thermal conductivity, but little has been shown regarding the effect of the metal additives on the overall system performance. This section investigates the effect of different

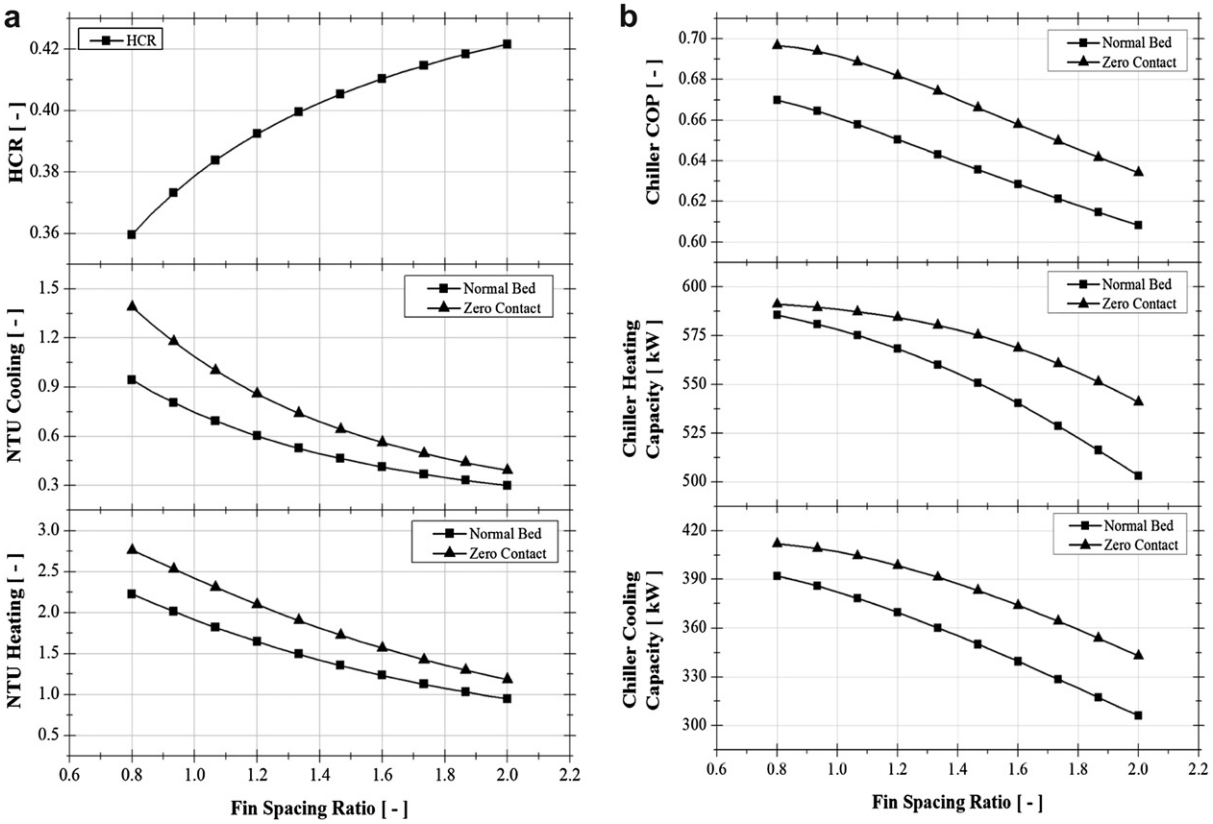

Fig. 4. Effects of eliminating contact resistance on adsorbent-bed thermal performance (a) and chiller overall performance (b) at various fin spacing ratio.

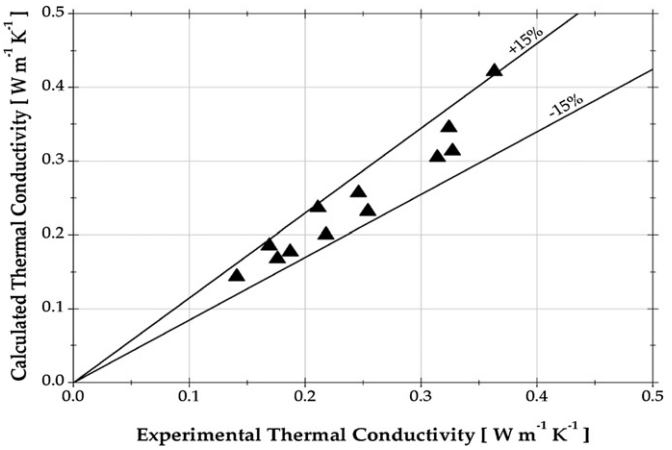

Fig. 5. Predicted thermal conductivity versus experimental values of Demir et al. [24].

metal additives on the overall performance of the 450 kW silica gel/water adsorption system.

Demir et al. [24] has experimentally investigated the effect of different metal additives (aluminium, copper, brass and stainless steel) on the thermal conductivity of unconsolidated packed silica gel bed using different silica gel/metal weight ratios (5, 10 and 15wt%). They used silica gel granules with 3–5 mm diameter and thermal conductivity of 0.106 W m^{-1} K^{-1}, while the radius of the frontal area of the metal particles was 1–2.8 mm. The volume based two phase effective thermal conductivity (K) method was used to develop a prediction technique for the thermal conductivity of silica gel/metal particles mixture, Eq. (8).

$$K = [k_1 V_1 (dT/dx)_1 + k_2 V_2 (dT/dx)_2] / [V_1 (dT/dx)_1 + V_2 (dT/dx)_2] \quad (8)$$

where k_1 and V_1 are the thermal conductivity and volume fraction of metal respectively, while k_2 and V_2 are thermal conductivity and volume fraction of silica gel respectively. The overall average temperature gradient $(dT/dx)_1$ and $(dT/dx)_2$ of the two phases were determined as:

$$(dT/dx)_1 / (dT/dx)_2 = nk_1 / [k_2 + (n-1)k_1] \quad (9)$$

Factor n depends mainly on the metal additive shape [26]. Using factor n of 1.031, 1.047, 1.11 and 2.331 for aluminium, copper, brass and stainless steel metal additives respectively and various metal/silica gel mass ratio (5%, 10% and 15wt%), the effective thermal conductivity of silica gel/metal mixture can be predicted. Fig. 5 compares the predicted thermal conductivity and the experimental values reported by Demir et al. [24] with deviation of less than ±15%. This validated prediction method was then used to calculate the effective thermal conductivity of the metal/silica gel mixtures shown in Table 3 using silica gel type-RD2060 with thermal conductivity and average granules diameter of 0.198 W m^{-1} K^{-1} and 0.16 mm respectively [25].

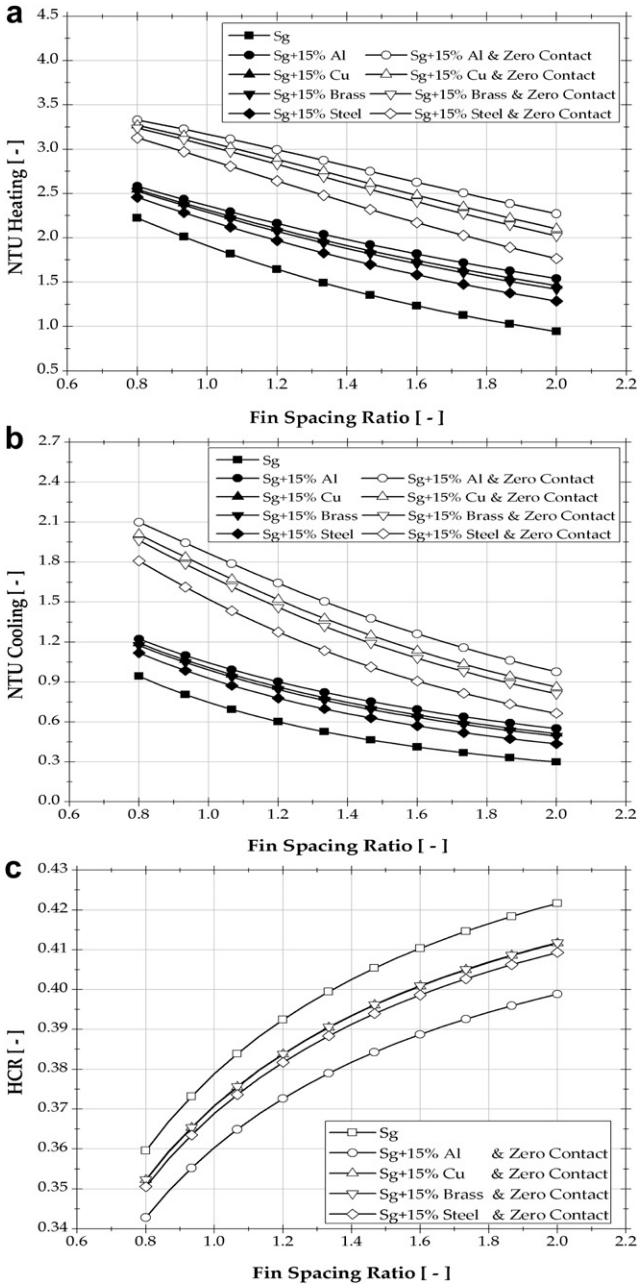

Fig. 6. The effect of metal additives on adsorbent-bed thermal performance.

Table 3
The predicted metal/silica gel type-RD effective thermal conductivity.

Met/Sg mixture	K_{met} (W m^{-1} K^{-1})	K_{eff} (W m^{-1} K^{-1})	Thermal conductivity improvement (%)
Silica gel	–	0.198	–
Sg+5% Al	237	0.340	72
Sg+10% Al	237	0.498	152
Sg+15% Al	237	0.675	241
Sg+5% Cu	401	0.305	54
Sg+10% Cu	401	0.424	114
Sg+15% Cu	401	0.557	181
Sg+5% Brass	150	0.291	47
Sg+10% Brass	150	0.394	99
Sg+15% Brass	150	0.509	157
Sg+5% St–St	14.9	0.254	28
Sg+10% St–St	14.9	0.316	60
Sg+15% St–St	14.9	0.385	94

The predicted effective thermal conductivities of metal/silica gel RD2060 were incorporated in the overall chiller model. Fig. 6 presents the effects of aluminium, copper, brass and stainless steel metal additives of 15wt% on the adsorbent-bed thermal performance at various fin spacing. It is observed that the adsorbent-bed NTU during heating averagely increased by 39.5%, 34.7%, 32.2% and 23.8% and during cooling by 58.2%, 50.2%, 46.3% and

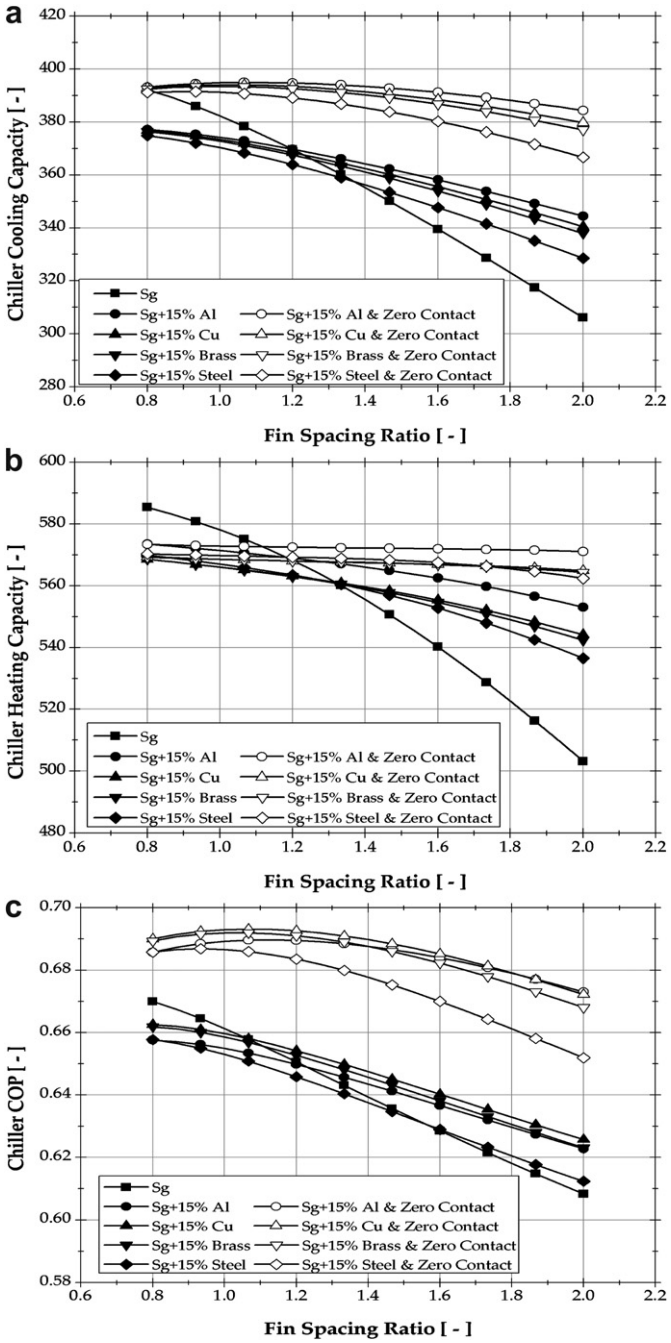

Fig. 7. The effect of metal additive on chiller overall performance.

33.3% using aluminium, copper, brass and stainless steel respectively. On the other hand, the heat capacity ratio of the adsorbent bed averagely decreased by 5.1%, 2.2%, 2.2% and 2.7% using aluminium, copper, brass and stainless steel additives respectively. The decrease in HCR is due to the reduction of silica gel mass which was replaced with metal additives of different specific heats. Fig. 6(c) shows the HCR values of silica gel/metal additives mixture with zero contact resistance only since elimination of contact resistance does not affect the HCR values as indicated in section 4.

Fig. 7 shows the effect of the same metal additives on the chiller cooling capacity, heating capacity and COP. Results showed that the addition of metal particles at 15% wt enhanced the chiller cooling capacity and coefficient of performance at varying degree depending on the fin spacing ratio and the metal type. At FSR of 2, the cooling capacity, heating capacity and COP increased by 12.5%, 9.9% and 2.4% for aluminium, 11.2%, 8.1% and 2.9% for copper, 10.4%, 7.8% and 2.4% for brass and 7.3%, 6.6% and 0.7% for stainless steel. At FSR of 0.8, the cooling capacity, heating capacity and COP decreased by 3.8%, 2.0% and 1.8% for aluminium, 4.0%, 2.8% and 1.1% for copper, 4.1%, 2.9% and 1.2% for brass and 4.4%, 2.7% and 1.8% for stainless steel. It can be seen that Aluminium as a metal additive produced the highest improvement in system performance. This is due to the higher effective thermal conductivity of the silica gel/aluminium mixture as calculated by Eqs. (8) and (9) and presented in Table 3.

6. Effect of zero contact resistance and metal additives

Figs. 6 and 7 also show the combined effect of gluing the first layer of silica gel/metal particles on the adsorbent-bed reactor and chiller performance respectively. Results show that using both enhancement techniques (gluing the first adsorbent/metal mixture layer) increased the adsorbent-bed NTU during heating averagely by 89.5%, 81.2%, 77.0% and 63.2% and during cooling by 173.6%, 151.8%, 141.5% and 110.0% using aluminium, copper, brass and stainless steel respectively. Fig. 7 shows that the effect of the combined enhancement varies with the fin spacing ratio. At FSR of 2, the chiller cooling capacity and heating capacity increased 25.6%, 24.1%, 23.2%, 19.8% and 13.5%, 12.3%, 12.2%, 11.8% using aluminium, copper, brass and stainless steel respectively. Thus the system COP increased by 10.6%, 10.5%, 9.8% and 7.2% using aluminium, copper, brass and stainless steel respectively. However, at FSR of 0.8, the chiller COP increased only by 2.4%, 3%, 2.9% and 2.4% using aluminium, copper, brass and stainless steel respectively while the change in the cooling capacity was insignificant. The increase in the COP is due to the decrease in the heating capacity by 2.1%, 2.8%, 2.8% and 2.6% using aluminium, copper, brass and stainless steel respectively.

7. Conclusions

Literature review showed that there is potential for using various heat transfer enhancement techniques to improve adsorbent beds thermal performance. Most of this work mainly reports about enhancements in the thermal performance of the adsorbent materials. This work investigated theoretically some of the methodologies used to enhance the heat transfer performance of the adsorbent material in terms of improving the bed thermal performance and the overall cooling capacity of the adsorption system. In particular, the elimination of contact resistance, the use of metal additives and their combined effect were investigated using a validated thermal model of 450 kW commercially available water chiller.

Results showed that eliminating the contact resistance by sticking the first layer of adsorbent granules and packing the remaining ones averagely improves chillers cooling capacity and COP by 8.9% and 4.6% respectively.

Using different metal additives improves the heat transfer performance of adsorbent bed, up to 58.2% increase in the adsorbent-bed NTU during cooling with Aluminium additives which leads to 12.5% enhancement in the chiller cooling capacity at fin spacing ratio of 2. However, at lower fin spacing ratio (FSR$<$1.2), a negative enhancement was experienced which can be attributed to the increase in the ratio of metal to silica gel mass.

Results for the combined techniques showed that the enhancement in the cooling capacity increases with the increase in the fin spacing ratio to be maximum of 25% at FSR equals 2. Similar trend has been noticed for the COP where it reached a maximum of 10%.

The above results show the potential of using validated simulation models to investigate means of improving the performance of adsorption cooling systems.

Acknowledgements

The authors wish to thank Weatherite Holdings Ltd and the Engineering and Physical Science Research Council (EPSRC) for sponsoring this project.

Nomenclature

Symbol

A	Area (m^2)
C	Specific heat (kJ kg^{-1} k^{-1})
Cp	Specific heat capacity at constant pressure (kJ kg^{-1} k^{-1})
d	Diameter (m)
D_{so}	Pre-exponential constant (m^2 s^{-1})
dT/dx	overall average temperature gradient (K m^{-1})
ΔH	Isosteric heat of adsorption (kJ)
E	Energy (kJ)
E_a	Activation energy (J mol^{-1})
h	Specific enthalpy (kJ kg^{-1})
HCR	Heat capacity ratio
k	Thermal conductivity ($Wm^{-1}K^{-1}$)
K	Thermal conductivity ($Wm^{-1}K^{-1}$)
LMTD	Logarithmic mean temperature difference (K)
M	Mass (kg)
$\dot{m}$	Mass flow rate (kg s^{-1})
n	Metal additives factor
NTU	Number of transfer unit
P	Pressure (kPa)
R	Universal gas constant (J mol^{-1} K^{-1})
R_{cont}	Contact thermal resistance (W m^{-1} K^{-1})
R_p	Particle radius (m)
T	Temperature (K)
t	Time (s)
U	Overall heat transfer coefficient (kWm^{-2} K^{-1})
V	Volume fraction
w	Uptake value (kg kg^{-1})
w^*	Equilibrium uptake (kg kg^{-1})

Greek symbols

Σ	Summation
Φ	Flag
δ	Flag
ξ	Flag
γ	Flag

Subscripts

ads	Adsorbent
cond	Condenser
evap	Evaporator
f	Liquid
g	Vapour
i	Inside
met	Metal
o	Outside
r	Root
ref	Refrigerant
sat	Saturation
sg	Silica gel
t	Tube
w	water

References

[1] R.E. Critoph, Evaluation of alternative refrigerant-adsorbent pairs for refrigeration cycles, Applied Thermal Engineering 16 (1996) 891–900.
[2] S. Li, J.Y. Wu, Theoretical research of a silica gel-water adsorption chiller in a micro combined cooling, heating and power (CCHP) system, Applied Energy 86 (2009) 958–967.
[3] H. Luo, R. Wang, Y. Dai, The effects of operation parameter on the performance of a solar-powered adsorption chiller, Applied Energy 87 (2010) 3018–3022.
[4] C.J. Chen, R.Z. Wang, Z.Z. Xia, Study on a compact silica gel-water adsorption chiller without vacuum valves: design and experimental study, Applied Energy 87 (2010) 2673–2681.
[5] R.K. Aldadah, A.R.M. Rezk, Empirical simulation model of silica gel/water adsorption chiller, in: ASME-ATI-UIT, Thermal and Enviromental Issues in Energy Systems (2010) (Sorrento, Italy).
[6] A. Freni, L. Bonaccorsi, E. Proverbio, Zeolite synthesised on copper foam for adsorption chillers: a mathematical model, Microporous and Mesoporous Materials 120 (2009) 402–409.
[7] G. Restuccia, A. Freni, G. Maggio, A zeolite-coated bed for air conditioning adsorption systems: parametric study of heat and mass transfer by dynamic simulation, Applied Thermal Engineering 22 (2002) 619–630.
[8] T.-H. Eun, H.-K. Song, J.H. Han, Enhancement of heat and mass transfer in silica-expanded graphite composite blocks for adsorption heat pumps. Part II. Cooling system using the composite blocks, International Journal of Refrigeration 23 (2000) 74–81.
[9] L. Wang, D. Zhu, Y. Tan, in: Heat Transfer Enhancement on the Adsorber of Adsorption Heat Pump, vol. 5, Springer, Netherlands, 1999, pp. 279–286.
[10] T.-H. Eun, H.-K. Song, J. Hun Han, Enhancement of heat and mass transfer in silica-expanded graphite composite blocks for adsorption heat pumps: part I. Characterization of the composite blocks, International Journal of Refrigeration 23 (2000) 64–73.
[11] S.G. Wang, R.Z. Wang, X.R. Li, Research and development of consolidated adsorbent for adsorption systems, Renewable Energy 30 (2005) 1425–1441.
[12] P. Hu, J.-J. Yao, Z.-S. Chen, Analysis for composite zeolite/foam aluminum-water mass recovery adsorption refrigeration system driven by engine exhaust heat, Energy Conversion and Management 50 (2009) 255–261.
[13] L. Bonaccorsi, A. Freni, E. Proverbio, Zeolite coated copper foams for heat pumping applications, Microporous and Mesoporous Materials 91 (2006) 7–14.
[14] A. Freni, B. Dawoud, F. Cipiti, Finite element-based simulation of the heat and mass transfer process through an adsorbent bed in an adsorption heat pump/chiller, in: ASME-ATI-UIT, Conference on Thermal and Environmental Issues in Energy Systems (2010) (Sorrento, Italy).
[15] A.R.M. Rezk, R.K. Al-Dadah, Physical and operating conditions effects on silica gel/water adsorption chiller performance, Applied Energy (2011). doi:10.1016/j.apenergy.2010.11.021.
[16] G. Cacciola, G. Restuccia, G.H.W. van Benthem, Influence of the adsorber heat exchanger design on the performance of the heat pump system, Applied Thermal Engineering 19 (1999) 255–269.
[17] G. Cacciola, G. Restuccia, Progress on adsorption heat pumps, Heat Recovery Systems and CHP 14 (1994) 409–420.
[18] S.D. Waszkiewicz, M.J. Tierney, H.S. Scott, Development of coated, annular fins for adsorption chillers, Applied Thermal Engineering 29 (2009) 2222–2227.
[19] G. Restuccia, G. Cacciola, Performances of adsorption systems for ambient heating and air conditioning, International Journal of Refrigeration 22 (1999) 18–26.
[20] K.-S. Chang, M.-T. Chen, T.-W. Chung, Effects of the thickness and particle size of silica gel on the heat and mass transfer performance of a silica gel-coated bed for air-conditioning adsorption systems, Applied Thermal Engineering 25 (2005) 2330–2340.
[21] H. Demir, M. Mobedi, S. Ulku, A review on adsorption heat pump: problems and solutions, Renewable & Sustainable Energy Reviews 12 (2008) 2381–2403.
[22] U. Jakob, W. Mittelbach, Development and investigation of a compact silica gel/water adsorption chiller integrated in solar cooling systems, in: VII Minsk International Seminar (2008).
[23] L. Schnabel, M. Tatlier, F. Schmidt, Adsorption kinetics of zeolite coatings directly crystallized on metal supports for heat pump applications (adsorption kinetics of zeolite coatings), Applied Thermal Engineering 30 (2010) 1409–1416.
[24] H. Demir, M. Mobedi, S. Ülkü, The use of metal piece additives to enhance heat transfer rate through an unconsolidated adsorbent bed, International Journal of Refrigeration 33 (2010) 714–720.
[25] X. Wang, W. Zimmermann, K.C. Ng, Investigation on the isotherm of silica gel+water systems TG and volumetric methods, Journal of Thermal Analysis and Calorimetry 76 (2004) 659–669.
[26] R.I. Hamilton, O.K. Crosser, Thermal conductivity of hetrogeneous two-component systems, Industrial and Engineering Chemistry Fundamentals 1 (1962) 187–191.